Modeling and simulation methodology for digital optical computing systems

Ahmed Louri and Jongwhoa Na

A modeling and simulation methodology for digital optical computing systems is introduced in this paper. The methodology predicts maximum performance of a given optical computing architecture and evaluates its feasibility. As an application example, we apply this methodology to evaluate the feasibility and performance of the optical content-addressable parallel processor proposed in Appl. Opt. **31,** 3241 (1992). The approach consists of two major phases. The first phase involves analytical studies of the effects of design parameters such as cross talk, diffraction-limited beam spot diameter, and pitch on system performance parameters such as signal packing density and skew time. In the second phase, a simulation model and a simulator are introduced by the use of GLAD (General Laser Analysis and Design, an optical software package developed by Applied Optics Research) to evaluate the combined effects of bit-error rate, bit rate, optical power efficiency, available source power, and signal contrast on the performance parameters such as signal packing density, misalignment tolerance, and distance between devices. The methodology presented here investigates the model, not on a component-by-component basis, but as a whole, which produces a more realistic representation of the actual laboratory prototype. The proposed methodology is intended to reduce the optical computing system design time as well as the design risk associated with building a prototype system.

Key words: Digital optical computing, diffraction analysis, modeling and simulation, optical content-addressable parallel processor.

1. Introduction

In recent years, several optical computing architectures and systems have been proposed.[1–6] These systems are designed to exploit the advantages of optics such as noninterference between signals, inherent parallelism, and high spatial and temporal bandwidth. Although some of the proposed systems present results of laboratory prototypes and some report results based on first-order analysis, the systematic or automated modeling and simulation methodologies have not yet been presented. Without the aid of a general-purpose simulation model, the development periods from an initial concept of an actual prototype have been too long, and the accompanying costs have been too high. One study showed that the conceptual design, engineering design, fabrication, and testing of an optical system typically takes 3–5 years.[7] Moreover, problems arise when the target system becomes so complex that there are simply too many parameters to be considered. As the optical computing and networking systems gain popularity, future systems will become increasingly complicated. Therefore it is necessary to have automated optical system design and analysis tools.

In optical system research fields other than optical computing, the importance of these automated tools is already recognized. For example, an optical disk storage system that utilizes a laser diode head and an optical disk has been modeled and simulated.[8] An integrated design tool called SCOPE (supercompact optoelectronic simulator) has been proposed[9] for microwave optoelectronic systems that handle laser diodes, light-emitting diodes, and photodetectors. In the optical interconnection network field, several researchers have reported the modeling and simulation study of optical interconnects.[10,11] For optical computing systems, up until now, there have been no modeling and simulation tools for verifying the proper functionality of an optical computing system as well as its physical realizability. We should note that some efforts have been made to design computer-aided designs (CAD's) for optical computing systems,[12,13] but these efforts have been limited to only the functional aspects of systems.

The authors are with the Department of Electrical and Computer Engineering, University of Arizona, Tucson, Arizona 85721.

Received 20 May 1993; revised manuscript received 20 September 1993.

0003-6935/94/081549-10$06.00/0.

In this paper we propose a modeling and simulation methodology for digital optical computing systems that not only evaluates the feasibility of the system but also tests its functionality and predicts its performance. As an application example, we apply the proposed methodology to the optical content-addressable parallel processor[14] (OCAPP). The approach consists of two major phases. In the first phase, analytical studies are performed to investigate the effects of design parameters such as cross talk (including power dissipation and noise), diffraction-limited beam spot diameter, and pitch on signal packing density, skew time (execution time), and system volume. In the second phase a simulation model and a simulator are introduced to evaluate the combined effects of bit-error rate (BER), bit rate (BR), optical power efficiency, and available source power on the performance parameters such as maximum signal packing density, misalignment tolerance, and maximum distance between devices. The simulator is designed by the use of GLAD (General Laser Analysis and Design, an optical simulation software package developed by Applied Optics Research[15]). GLAD permits detailed modeling of each system component of systems such as spatial light modulators (SLM's) in addition to simulating the propagation of an optical wave front passing through them. The proposed approach enables a more complete evaluation of the conceptual design, which will eventually result in faster prototype development.

The rest of this paper is organized as follows: Section 2 presents a brief description of the OCAPP and GLAD. Section 3 proposed a modeling and simulation methodology for the OCAPP. Section 4 characterizes the performance of the diffraction-limited OCAPP. Section 5 describes how GLAD is used to simulate the OCAPP and the values of the parameters considered. Section 6 summarizes the simulation work, and Section 7 concludes the paper.

2. Background

A. Modeling and Simulation

In this subsection we briefly discuss the underlying concepts of modeling and simulation. Modeling and simulation of a system is a technique that acts as a bridge between a conceptual design and a laboratory prototype. In an abstract sense, modeling means collecting all possible information about a system. This information collection process may be accomplished either by coding the structure and the behavior of the optical system by the use of conventional programming languages such as C or PASCAL or by the use of optical system analysis software packages such as CODE V, OSLO, or GLAD.[16,17]

Simulation may be defined as an experiment performed on a model. In computer system simulation, two aspects can be noted, namely the functional and the physical aspects. The simulation of functionality means verifying the functions or algorithms that are going to be performed on the system. It is typically done by using conventional programming languages or simulation packages such as DEVS (Discrete EVent-based Simulation) or SIMSCRIPT.[18,19] The simulation of the physical aspect of a computer system means verifying the physical realizability of the conceptual design. This can be done by simulating each component of the computer system by the use of an optics simulation or a ray-tracing software package.

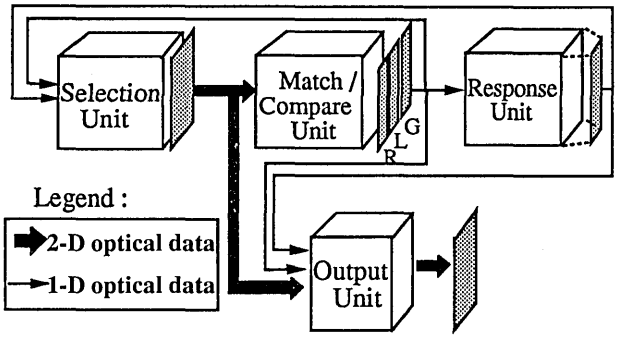

Fig. 1. Architecture of the OCAPP.

B. Optical Content-Addressable Parallel Processor

In Ref. 14, a parallel architecture called the OCAPP has been introduced for the fast and efficient implementation of symbolic computing tasks such as searching, sorting, information retrieval and database–knowledge-base processing. Figure 1 is a schematic diagram of the OCAPP. The architecture is composed of a selection unit, a match/compare unit, a response unit, an output unit, and a control unit, the words stored in the storage array. A detailed explanation and implementation of each unit of the OCAPP and the algorithms implemented on the OCAPP are presented in Ref. 14.

This architecture is under construction in the Optical Computing and Parallel Processing Laboratory at the University of Arizona. A laboratory setup is shown in Fig. 2. The optical system is composed of three SLM's, a beam splitter, spherical and cylindrical lens elements, spatial filtering assemblies, mirrors, and two linear CCD (charge-coupled device) arrays. The OCAPP uses a collimated laser

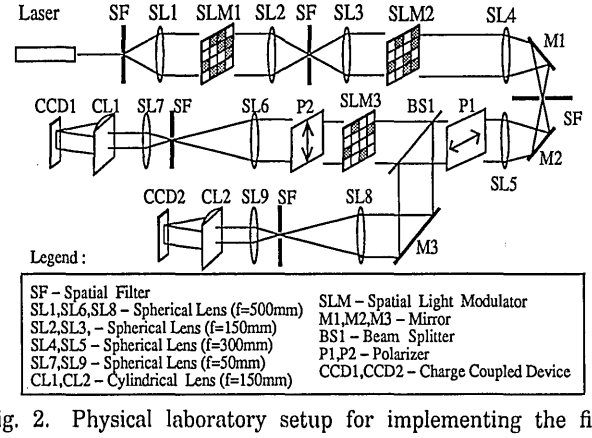

Fig. 2. Physical laboratory setup for implementing the first version of the OCAPP.

beam as an input source and two linear CCD arrays as the output detection unit. The operations of the match/compare unit are performed by SLM1 and SLM2. SLM1 and SLM2 are used to hold two words or two bit slices to be matched or compared with respect to each other, depending on the algorithm employed. The selection unit is mapped into SLM3, which is used to enable/disable words and/or bit-slices of the two-dimensional (2-D) optical data array from SLM2. The response unit is omitted in this layout because the first version of the OCAPP is configured as a relational database machine, which does not use ordering between the matched words.

The optical layout for OCAPP architecture is further simplified into a simulation model, shown in Fig. 3. This model is more suitable for the simulation study without loss of functionality of the original OCAPP described in Ref. 14. The simulation model of Fig. 3 constitutes the major optical path of the system of Fig. 2 that consumes most of the power. For clarity, the spatial filtering assembly and mirrors are not considered in the simulation model as they contribute little power loss in our application. This modified OCAPP model is studied with the simulation methodology described in Section 3.

C. General Laser Analysis and Design

There are two types of commercial software package for the analysis and design of optical systems. One is a geometric code (such as CODE V[16] or OSLO[17] that is based on ray-tracing optics, and the other is a physical optics code (such as GLAD)[20] that is based on diffraction propagation of wave fronts. Although geometric codes may be useful in analyzing the given system to some extent, the physical optics code is able to provide a more accurate and powerful tool by utilizing fast Fourier transforms.[21] The physical optics code provides detailed beam intensity and phase profiles, whereas the geometric code is limited to providing simple intensity profiles such as a constant or Gaussian profile.[21] Moreover, the geometric code limits the diffraction propagation to strictly near field or far field, whereas the physical code can handle any kind of diffraction propagation. For the above reasons, we chose to use GLAD for our purpose.

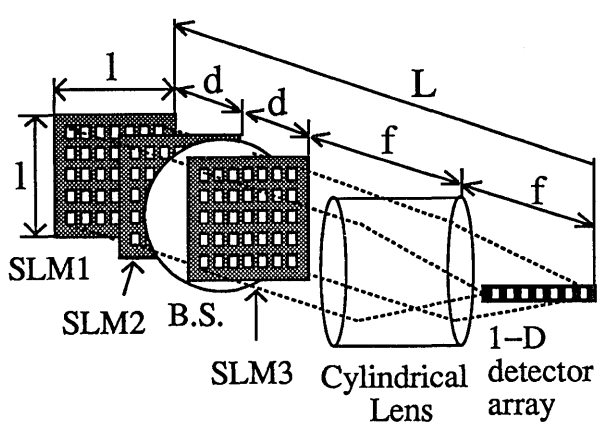

Fig. 3. Simplified model of the OCAPP.

3. Modeling and Simulation of the Optical Content-Addressable Parallel Processor

In this section, a two-phase modeling and simulation methodology for digital optical computing systems is proposed, and the simulation results are explained. The main objectives of the methodology are finding maximum values of performance parameters of a given optical computing system as well as providing a laboratory prototype model for fast prototype development. Performance parameters considered here include signal packing density, misalignment tolerances, distance between components, power efficiency, and skew time.[22,23] Maximum values can be found by manipulating cross talk, BER, BR, and optical power efficiency of a given system. During the first phase, a theoretical analysis of the system is performed. During the second phase, GLAD is used for a detailed simulation and evaluation of the system. In what follows, we describe each phase in detail.

A. Phase 1: Diffraction Analysis of the Optical Content-Addressable Parallel Processor

In the first phase, a preliminary analysis is performed to narrow down the range of values of parameters used in the simulation. The analysis provides upper bounds of performance parameters such as diffraction-limited signal packing density, skew time, and cross talk. Knowing these bounds would enable one to avoid unnecessary simulation experiments and to have a better understanding of the overall simulation work. Another point to note is that some parameters identified at the preliminary analysis phase can be used in the second phase. For example, skew time, which is estimated in the first phase, is used in the calculation of the BR that is used in evaluating the required optical input power. A summary of parameters and definitions used in this paper is given in Table 1.

In the first phase, the pitch, signal power, noise power, cross talk, and diffraction-limited beam spot diameter are used as design parameters that can be manipulated whereas the signal packing density is used as a performance parameter. First, the diffraction-limited signal packing density is calculated by obtaining the minimum pitch for a given system cross talk. The cross talk is expressed in terms of the pitch. This is possible because the cross talk is the ratio of the noise power to the signal power, and the noise power can be expressed in terms of pitch. The noise power is obtained by integrating the output intensity distribution over the neighboring detector apertures. The neighboring detector aperture can be expressed in terms of the diffraction-limited beam spot diameter and pitch. The skew time is obtained by calculating the difference between the maximum and the minimum optical path lengths. The skew time is then used to estimate the cycle time and maximum bit rate of the OCAPP. Finally, the volume of the OCAPP and optical power dissipation-limited signal packing density are calculated. In

Table 1. List of the Parameters Used

Symbol	Definition
a	Length of a pixel of a SLM
d_D	Diffraction-limited beam spot diameter
n	Number of pixels per row (or column)
p	Pitch: center-to-center distance between two adjacent pixels
ρ	Signal packing density: number of pixels per 1 cm^2
η_t	System optical power efficiency
d	Distance between SLM's
f	Cylindrical lens focal length
λ	Optical wavelength
l	Length of the SLM
L	Length of the system
N	System fanout
N_f	Fresnel number
T_{skew}	Skew time: propagation time difference from input to output among the various optical paths
v	Volume of the system
BER	Bit error rate
BR	Bit rate
χ	Cross talk: ratio of noise power to signal power
P_{in}	Required optical power per beam
P_{signal}	Collected optical power at the designated detector element
P_{noise}	Collected optical power at the detectors other than the designated detector element
Q	Ratio of the rms signal voltage to the total rms cross-talk voltage
r	Ratio of current to the detector in the OFF state over the ON state
σ_p	Power dissipation density (in watts per square centimeter)

what follows, the parameters in Phase 1 are calculated based on the architecture shown in Fig. 3.

1. Diffraction-Limited Beam Spot Diameter

The diffraction-limited beam spot diameter d_D for a given system configuration is calculated here. d_D will be used below for the optical signal power calculation. In order to check the extreme case, we assume that the SLM's, beam splitter, and cylindrical lens are in contact. In the case of square input aperture, d_D is given by

$$d_D = \frac{2\lambda f}{a}, \tag{1}$$

where a is the length of a pixel of the SLM, f is the focal length of the cylindrical lens, and λ is the laser wavelength (refer to Fig. 3). For simplicity, we assume that the lengths of the pixel on the SLM and that of a detector have the same value, which is a. Then d_D becomes

$$d_D = a = \sqrt{2\lambda f}. \tag{2}$$

2. Diffraction-Limited Signal Packing Density

The signal packing density ρ is one of the most important performance parameters as it limits the maximum number of pixels in the optical data plane. In order to determine the maximum signal packing density ρ_M, the individual pixels must be packed as tightly as possible. Therefore ρ_M is obtained by finding the minimum pitch p_m of the 2-D array.

The pitch p can be related to the cross talk χ calculation because the cross-talk calculation requires the evaluation of the collected noise power P_{noise}, which uses p as an integration parameter. In other words, to calculate P_{noise}, the intensity distribution must be integrated over the neighboring detector aperture, which has a diameter of d_D, and separated from the designated detector aperture by multiples of p.[24,25] Therefore, by setting χ to some value, we can calculate p_m of the array. Once p_m is known, we can directly calculate ρ_M and the maximum number of pixels in the array.

To calculate χ, we calculate the field distribution at the output plane $u_2(x, y)$ of a pixel located at the center of the input plane (SLM1 of Fig. 3) for a given input field distribution $u_1(x, y)$. As we have a collimated laser beam as a source, $u_1(x, y)$ can be approximated as a normally incident unit amplitude plane wave. Assuming a square aperture for the SLM pixel, the field distribution immediately after the square pixel of dimension a is given by

$$u_1(x, y) = \text{rect}(x/a, y/a) = \text{rect}(x/a)\text{rect}(y/a). \tag{3}$$

Because the rect function is separable and the power of the lens exists only along the y axis, the output distribution at the y axis will be a Fraunhofer diffraction pattern that can be expressed as

$$u_2(y) = \frac{\exp(jkz)\exp(jkx^2/2z)}{j\lambda z}\, a\, \text{sinc}\left(\frac{ay}{\lambda z}\right). \tag{4}$$

The output field distribution $u_2(x)$ along the x axis will be a Fresnel diffraction pattern as there is no focal power in the x direction in the cylindrical lens:

$$u_2(x) = \frac{\exp(jkz)}{j\lambda z}\int_{-a/2}^{a/2} \exp\left[j\frac{k}{2z}(x_1 - x)^2\right]dx_1. \tag{5}$$

Now we check the Fresnel number N_f, which is defined to be $a^2/\lambda f$, to study $u_2(x)$. For the following estimation, we assume that we have $\lambda = 633$ nm and $f = 0.1$ m. For the given λ and f, with Eq. (2), a becomes 356 μm. With the above data, N_f becomes ~ 2. This number implies that the diffraction pattern of $u_2(x)$ will be neither a geometric projection of aperture function nor the Fraunhofer diffraction pattern. Figure 4 shows the intensity distribution of the diffraction pattern of $u_2(x)$, which we calculated by solving Fresnel integrals at the cylindrical lens focal plane. Next we calculate χ between channels. Figure 5 shows the geometry used in the signal and noise power calculation. The parameter χ can be defined as

$$\chi = \frac{\Sigma P_{noise}}{P_{signal}}, \tag{6}$$

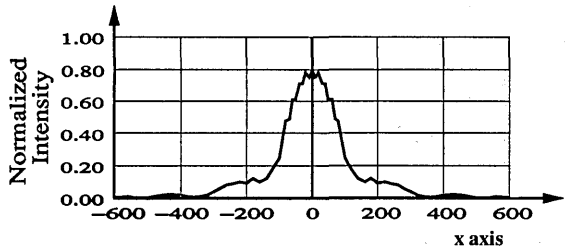

Fig. 4. Intensity distribution of the Fresnel diffraction pattern of a square aperture of a SLM. The dimension of a pixel is 356 μm × 356 μm.

where P_{signal} is the power collected over the center pixel (pixel A of Fig. 5) of the detector (assuming pixel A is the intended destination). The signal power collected at pixel A is

$$P_{\text{signal}} = \int_{-d_D/2}^{d_D/2} \int_{-d_D/2}^{d_D/2} I(x, y)\mathrm{d}x\mathrm{d}y. \tag{7}$$

On the other hand, P_{noise} is the power collected by the neighboring detector elements around the intended detector element. For simplicity, if we include only two neighboring detector elements (pixel B and pixel C of Fig. 5) in our calculation, P_{noise} is given by

$$\Sigma P_{\text{noise}} \simeq 2P_{n1}, \tag{8}$$

where P_{n1} is the power obtained from the closest neighboring pixel and can be calculated as

$$P_{n1} = \int_{-d_D/2}^{d_D/2} \int_{p-d_D/2}^{p+d_D/2} I(x, y)\mathrm{d}x\mathrm{d}y, \tag{9}$$

where p represents the pitch between pixels. For P_{n1} calculation, $I(x)$ (the Fresnel diffraction pattern) is integrated over the integration interval $p \pm d_D/2$ along the x axis at the cylindrical lens focal plane.

Figure 6 shows the calculated cross talk for various pitches when d_D is fixed at 356 μm, $\lambda = 633$ nm, and $f = 0.1$ m. Once the pitch is found, as shown in Fig. 7, the signal packing density can be estimated with the following relation[25]:

$$\rho = 1/p^2. \tag{10}$$

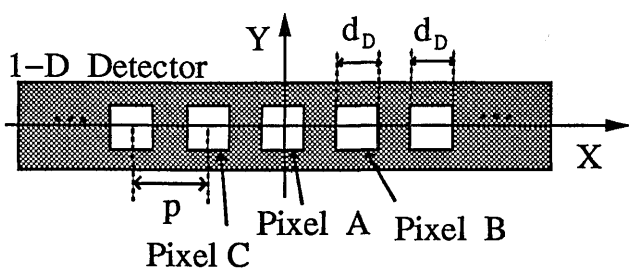

Fig. 5. Model of the detector aperture used for estimating the cross talk.

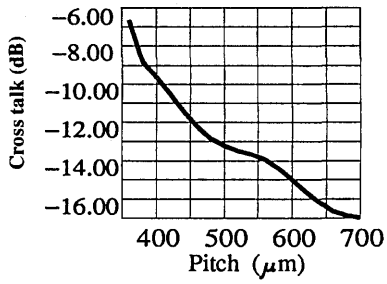

Fig. 6. Cross talk for various pitches of the SLM array in the diffraction-limited OCAPP. Diffraction-limited beam spot diameter is set to 356 μm.

From Fermat's principle, light takes the shortest path between two points. As the OCAPP has a 3-D structure, there are inherent path-length differences between pixels of the input and the output optical data planes. This path-length difference generates a clock skew problem that can affect the accuracy as well as the operating speed of the optical computing system. This problem will be aggravated in systems in which the output signals are designed to be fed back to the input stage. Therefore, to calculate the operating speed of the OCAPP and avoid the above problems, we must identify the skew time of the system and the longest signal path to satisfy the synchronization requirement.[26]

In Fig. 3, the three SLM's perform imaging operations. Assuming that the length of the OCAPP is L (from SLM1 to the detectors) and that l is the length of an SLM, the time taken to travel the shortest path of the system, if the switching time of the SLM's is ignored, is given by

$$T_{\text{min}} = L/c. \tag{11}$$

On the other hand, the time taken to travel the longest path is given by

$$T_{\text{max}} = \frac{(L - f) + [(l/2)^2 + f^2]^{1/2}}{c}. \tag{12}$$

Therefore the skew time T_{skew} is

$$T_{\text{skew}} = T_{\text{max}} - T_{\text{min}} = \frac{[(l/2)^2 + f^2]^{1/2} - f}{c} = \frac{l}{2c}. \tag{13}$$

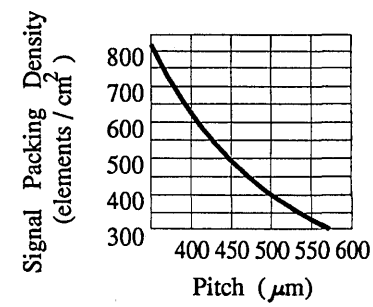

Fig. 7. Diffraction-limited estimation of signal packing density of the SLM versus the pitch.

It should be noted that $l = np$, where n is the number of pixels per row (or column) of the SLM, and p is the pitch. Substituting $l = np$ into Eq. (13) yields

$$T_{\text{skew}} = \frac{np}{2c}. \tag{14}$$

It can be seen that the skew time grows linearly with the number of pixels per dimension.

3. System Volume

The volume of an optical system affects the ease of packaging as well as the feasibility of the system. As SLM's are connected by imaging, the length of the OCAPP L from Fig. 3 is given by

$$L = 2d + 2f, \tag{15}$$

where d is the distance between two SLM's and f is the focal length of the cylindrical lens. The system volume v is given by

$$v = Ll^2 = 2(d + f)l^2 = 2(d + f)(np)^2. \tag{16}$$

It can be seen that the volume is proportional to the square of the number of pixels per dimension.

4. Power Dissipation-Limited Signal Packing Density

Now we consider the effect of power dissipation density on the signal packing density. It is known that the maximum intensity of the beam is limited by the maximum real power dissipation density σ_p, which has a typical value of 1 W/cm^2.[25,27] Then the maximum allowable heat dissipation per input beam, P_{crit}, is

$$P_{\text{crit}} = \frac{\sigma_p}{\rho}. \tag{17}$$

As shown by Ref. 25, it is σ_p that limits signal packing density more severely than diffraction effects. Even for low threshold lasers currently available, a threshold current of 1 mA is required for minimal operation. Assuming that laser operation requires ~3 mW per beam, then, for σ_p = 1 W/cm^2, ρ becomes 333 pixels/cm^2. For an SLM of 2 cm × 2 cm active area, the maximum number of pixels available on the SLM becomes 1332 pixels. Table 2 summarizes the results obtained from the analysis phase.

Table 2. Summary of Parameters Studied in the Analysis Phase

Design Parameter	Assumed Value	Calculated Parameter	Value
Cylindrical lens focal length f	10 cm	Diffraction-limited spot diameter d_D	356 μm
Length of SLM l	1.6 cm	Minimum pitch p_m	410 μm
System cross talk χ	−10 dB	Diffraction-limited signal packing density ρ	594 pixels/cm^2
Wavelength λ	633 nm	Power dissipation density-limited ρ	333 pixels/cm^2
Power dissipation density σ_p	1 W/cm^2	Skew time T_{skew}	26.67 ps
		Light propagation time T_{prop}	1.360 ns
		Volume v	25.6 cm^3

B. Phase 2: Modeling and Simulation of the Optical Content-Addressable Parallel Processor by the Use of GLAD

The second phase consists of modeling and simulating OCAPP. The main objective here is to provide a realistic evaluation of the system by providing the combined effects of design parameters on performance. Specifically, we would like to determine the maximum signal packing density, maximum misalignment tolerance, and maximum distance between devices for a given operating BR, BER, and optical power efficiency. As the GLAD model can provide a realistic representation of the model and simulate diffraction propagation of wave fronts by using 2^{20} observation points of the model, it is expected to generate the closest data to the prototype being built.

1. Modeling the Optical Content-Addressable Parallel Processor by the Use of GLAD

GLAD employs a modular-building-block approach to model each component in sequence as the beam propagates through the system.[15] The building-block approach permits a beam train of any configuration to be modeled by assembling blocks in the correct order. To design a simulation model for OCAPP, we must first model its components. Among the components of OCAPP, as shown in Fig. 3, the SLM is the most complicated component in the system. To model an SLM, we generate a prototype mask of a specific number of pixels, pixel size, pixel pitch, and physical dimension. Simulations are performed for systems that contain SLM's of varying signal packing densities. In order to maintain consistency among these various OCAPP models, the aggregate SLM dimension is held at a constant 1.6 cm × 1.6 cm size. For example, one of the models was a pixelated SLM consisting of 8 pixels × 8 pixels in a matrix configuration. This 8 × 8 SLM model determined the aggregate 1.6 cm × 1.6 cm dimension as the pixel pitch was 0.2 cm (i.e., the pixel size and the interpixel gap are both 0.1 cm). Then, for each specific bit pattern of the optical data plane of the SLM, the desired target pattern is overlaid on the prototype mask pattern. GLAD contains many commands to model components such as mirrors, lenses, apertures, etc. An initial field distribution for the beam by the use of geometric data such as the beam center, coordinates, waist size, and location can be defined with a command like GAUSSIAN. Once the optical configuration and the initial optical beam distribution are available, the

PROP (PROPagation) command is used to simulate diffraction propagation.

2. *Simulation of the Optical Content-Addressable Parallel Processor by the Use of GLAD*

a. Signal Packing Density. The simulation algorithm is illustrated in Fig. 8. Part-(A) of Fig. 8 describes the procedure for the maximum signal packing density ρ_M. The maximum signal packing density is obtained by simulating the model to obtain optical signal and noise power and calculating the required optical input power P_{in}. Once P_{in} is calculated, we compare it with the available optical source power. If the calculated P_{in} with a given signal packing density ρ is greater (less) than the available optical power, the model with a decreased (increased) ρ is prepared for the next simulation experiment.

In the following calculations, we set BER = 10^{-17}.[23] The BER can be represented as[27]

$$\mathrm{BER} = \frac{1}{\sqrt{2\pi}Q}\exp\left(\frac{-Q^2}{2}\right), \tag{18}$$

where Q is the ratio of the rms signal voltage to the total rms cross-talk voltage. For a given BER = 10^{-17}, $Q = 8.5$. For this given Q, the required optical input power P_{in} can be calculated as[28]

$$P_{in} = \frac{(1+r)}{(1-r)}\,Q\,\frac{h_c}{\lambda e}\,\langle i_{NA}{}^2\rangle^{1/2}\,\frac{N}{\eta_t}, \tag{19}$$

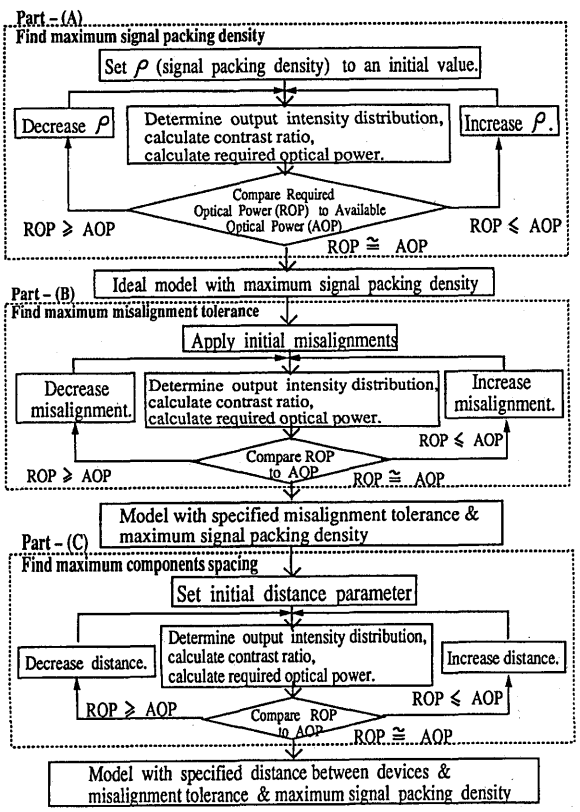

Fig. 8. Simulation algorithm for the OCAPP.

where r is the ratio of current to the detector in the low illumination state relative to the high illumination state, N is the system fan-out, η_t is the product of the quantum efficiency of the detector and the efficiency of the optical system, and $\langle i_{NA}{}^2\rangle^{1/2}$ is the rms current noise generated by the detector and preamplifier circuit.

Finally, to calculate P_{in}, we should determine the parameter r. As r represents the ratio of currents at the high illumination state to low illumination state, we obtain it by comparing the power incident upon the detector aperture at high and low illumination. The power for the two states is obtained by simulating the OCAPP model with a given SLM pixel pattern. To obtain power at the high illumination state, the desired pixel of each SLM is made transparent while others are set to opaque. Similarly, to obtain the power at the low illumination state, we set the pixels at the same column to opaque and make all the other pixels transparent. The whole column is cleared to avoid the effect of the cylindrical lens in the OCAPP. The factor $\langle i_{NA}{}^2\rangle$, which is expressed in terms of the BR, is calculated based on the data presented in Ref. 10, and N is set to 1 because of the one-to-one imaging between SLM's in the OCAPP. η_t is set to ~ 0.051 by considering a 50% ON-state power transmission efficiency for an ON-state pixel of the SLM, 50% power division at the beam splitter, and 4% reflection loss per surface (5 optical surfaces).

Once P_{in} is available, the number of pixels allowed per SLM can be obtained by comparing the required optical input power with the available source power. As shown in Part-(A) of Fig. 8, if the calculated power is less than (or greater than) the available power, a model with an increased (or decreased) number of pixels on the SLM plane is simulated. The maximum number of pixels is determined when the required optical input power is less than or equal to the available source power. The available optical power must be less than the actual power as there are other sources of power losses such as component misalignment and aberrations.

Figure 9 shows the optical power collected at the detector plane for models with various numbers of

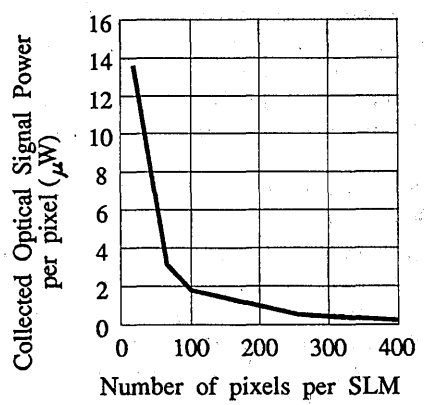

Fig. 9. Simulated detected optical signal power versus number of pixels of the optical data plane in the OCAPP.

pixels. The x axis of the graph represents the number of pixels of an SLM. The results of Fig. 9 are used to calculate P_{in}, as shown in Fig. 10. The simulation was started with the 4 × 4 model, which required 1.09-mW (68.19 μW × 4^2) optical source power. As a 5-mW He–Ne laser was selected as the source, the 8 × 8 model was simulated as the next step. The 8 × 8 model simulation requires 4.37 mW (68.23 μW × 8^2), which is still smaller than our source power. Next a 10 × 10 model was tested and found to require 7.33 mW (73.29 μW × 10^2), which exceeds the 5-mW requirement. Therefore the 8 × 8 model was selected for the simulation experiments. As a reference, a 20 × 20 model requires 57.04 mW (142.67 μW × 16^2).

b. Misalignment Tolerance. Once the maximum signal packing density for a given model becomes available, then the maximum misalignment tolerance is found by applying part-(B) of the procedure described in Fig. 8. To find the effects of misalignments on the optical collected signal and noise power, each individual misalignment is applied to each component of the model so that its effect on the collected optical power and required optical input power can be determined.

The procedure starts with the minimum resolvable misalignment. The unit of simulation is set to 50 μm. The unit of simulation means the distance between two sample data points used in the diffraction calculations, which are an adjacent pair among the 2^{20} data points. The minimum misalignment that can be applied becomes 50 μm.

Following part-(B) of Fig. 8, we extensively simulate the 8 × 8 model for misalignment tolerance. Figures 11 and 12 show the simulation result of required optical power. The two graphs show that up to 500 μm (half of a pixel width in the 8 × 8 model), the effect of applied lateral and longitudinal misalignments is not severe. However, as the amount of misalignment increases, the misalignment applied at SLM1 dominates the misalignment tolerance in both the x and the y directions. In the case of lateral misalignment, the maximum misalignment tolerance

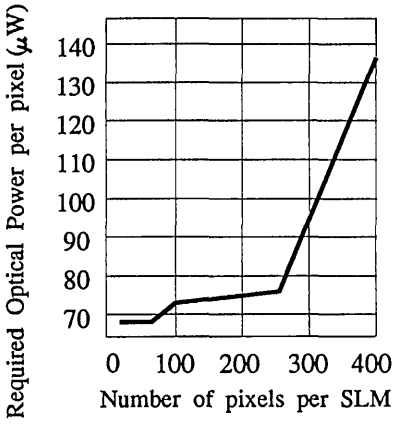

Fig. 10. Calculated required optical power P_{in} versus the number of pixels of the optical data plane in the OCAPP.

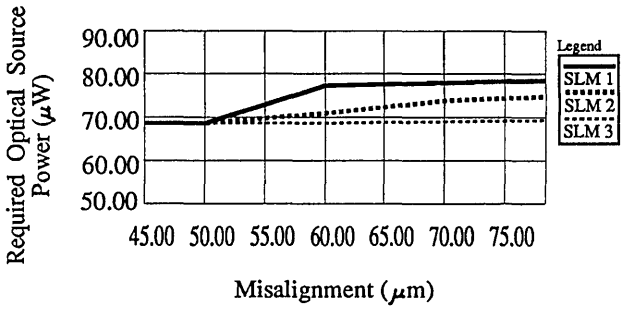

Fig. 11. Required optical power versus lateral misalignments applied.

becomes 700 μm. This value is obtained by comparing the line designated by SLM1 with the allowed beam power per pixel (5 mW/64 pixels = 78 μW). Also, for the longitudinal misalignment, the misalignment tolerance of 610 μm can be obtained from the graph.

c. Distance between Components. In optical computing systems, the mounting devices for optical components are important in that we must align tens or hundreds of individual beams with several devices. Also the beam broadens as it propagates because of the beam-spreading effect. Therefore, to enhance the signal integrity of the model, the distances between components must be minimized to the extent that mounting devices permit. From the system optimization perspective, we need to find the allowable range for d. This is calculated as shown in part-(C) of Fig. 8.

Figure 13 shows the required optical power of a 4 × 4, 8 × 8, 10 × 10, and 16 × 16 OCAPP for various values of d. The figure shows that for an 8 × 8 OCAPP, the change in the required optical power over various distances is almost indistinguishable. Therefore we can conclude that the 8 × 8 OCAPP is almost independent of the change in the distance between SLM's. However, as Fig. 13 shows, the required optical input power for larger OCAPP (16 × 16) increases exponentially with respect to the distance parameter.

4. Discussion

Table 3 summarizes the results obtained from the simulation phase. From the analysis of Phase 1 (the

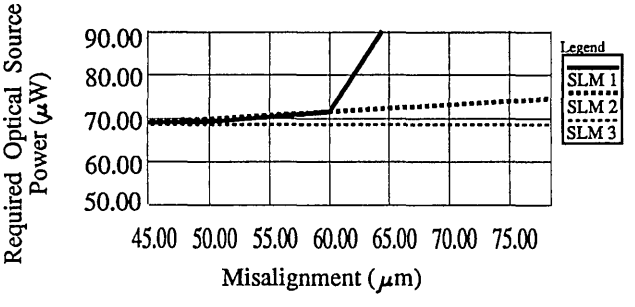

Fig. 12. Required optical power versus longitudinal misalignments applied.

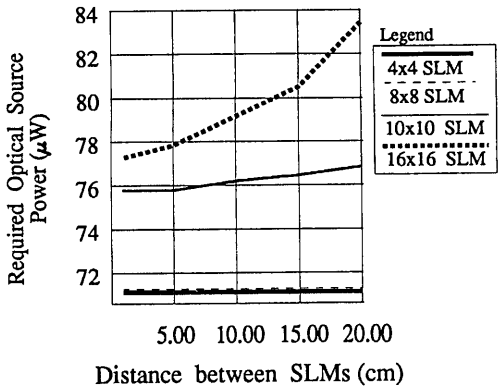

Fig. 13. Required power versus distance between SLM's.

results of which are summarized in Table 2), the theoretical upper bound of the maximum signal packing density is set by the heat removal capability. In addition to showing this heat removal factor, Table 3 shows that the input source power is also an important limiting factor in maximizing the signal packing density. To maximize the signal packing density, two directions may be pursued: first, proper device cooling techniques should be studied to increase the heat removal capacity, and second, optical sources such as surface-emitting laser diode arrays should be employed to deliver more power to the system.[29]

For misalignment, we found that the tolerance depends on the direction and the location in the system where misalignment occurred. For example, in the case of the 8 × 8 model simulation, misalignments occurring at SLM1 are crucial, and misalignments occurring at SLM2 and SLM3 are tolerable as long as the value of misalignment is less than the SLM pixel diameter. For SLM1, the lateral misalignment tolerance is found to be 700 μm, whereas the longitudinal misalignment tolerance is 610 μm. As the signal packing density increases (i.e., the pixel size decreases), the misalignment tolerance requirement will generally become more stringent.

For the distance between SLM's, the simulation of 4 × 4 and 8 × 8 OCAPP models showed that the distance between components is rather insensitive to the signal packing density. However, for larger signal packing density, (e.g., 10 × 10 or 16 × 16 models), the required optical power increases rapidly as the distance increases.

Table 3. Summary of Parameters Studied in the Simulation Phase

Design Parameter	Assumed Value	Simulated Parameter	Value
Laser power	5 mW	Signal packing density[a]	25 pixels/cm^2
SLM pixel size[a]	1000 μm	Lateral misalignment tolerance[a]	700 μm
Wavelength λ	633 nm	Longitudinal misalignment tolerance[a]	610 μm
System fanout N	1	Distance between SLM's[a]	20 cm
Optical power efficiency η_t	0.051		
BER	10^{-17}		
BR	0.75 Gbits/s		
Cylindrical lens focal length f	10 cm		
Length of SLM l	1.6 cm		

[a]This value is obtained from the 8 × 8 model simulation.

5. Conclusions

A modeling and simulation methodology is proposed to evaluate the performance as well as the feasibility of digital optical computing systems. As a particular example, the OCAPP is modeled and simulated. The proposed methodology integrates various system design parameters such as BER, BR, and optical power efficiency to determine maximum performance parameters such as maximum signal packing density, misalignment tolerance, and distance between components. In the analysis phase of the methodology, a diffraction-limited OCAPP model is examined to determine upper-bound values of design and performance parameters. Then in the simulation phase, a GLAD model is created and the model's performance parameters are investigated by extensive simulations. Following the proposed simulation methodology, the maximum signal packing density, misalignment tolerances, and the maximum distance between components are identified. The proposed methodology is intended to reduce optical computing systems' design time as well as the design risk associated with building the prototype system. The overall cost will also be reduced significantly because modeling and simulation permits design errors to be corrected before expensive and time-consuming prototype construction.

The authors thank G. N. Lawrence of the Optical Sciences Center, University of Arizona, for assistance in and permission for use of GLAD. This research was sponsored by National Science Foundation grant MIP-9113688.

References

1. A. Huang, "Architectural considerations involved in the design of an optical digital computer," Proc. IEEE **72,** 780–787 (1984).
2. A. A. Sawchuk and T. C. Strand, "Digital optical computing," Proc. IEEE **72,** 758–779 (1984).
3. J. Taboury, J. M. Wang, P. Chavel, and F. Devos, "Optical cellular processor architecture. 2: Illustration and system considerations," Appl. Opt. **28,** 3138–3147 (1989).
4. W. T. Cathey, K. Wagner, and W. J. Miceli, "Digital computing with optics," Proc. IEEE **77,** 1558–1572 (1989).
5. P. B. Berra, A. Ghafoor, M. Guizani, S. J. Marcinkowski and P. A. Mitkas, "Optics and supercomputing," Proc. IEEE **77,** 1797–1815 (1989).
6. M. E. Prise, N. C. Craft, M. M. Downs, R. E. LaMarche, L. A. D'Asaro, L. M. F. Chirovshy, and M. J. Murdocca, "Optical digital processor using arrays of symmetric self-electro-optic effect devices," Appl. Opt. **30,** 2287–2296 (1991).
7. J. R. Barry, "Knowledge-based environment for optical system design," in *1990 International Lens Design Conference,* G. N.

Lawrence, ed., Proc. Soc. Photo-Opt. Instrum. Eng. **1354,** 346–358 (1990).
8. J. P. Treptau, T. D. Milster, and D. G. Flagello, "Laser beam modeling in optical storage systems," in *Modeling and Simulation of Laser Systems II,* A. D. Schnurr, ed., Proc. Soc. Photo-Opt. Instrum. Eng. **1415,** 317–321 (1991).
9. T. Zhang, R. Hicks, and N. S. Tucker, "Simulator models lightwave systems at microwave rates," Microwaves Radio Freq. **30,** 114–119 (1991).
10. R. K. Kostuk, "Simulation of board-level free-space optical interconnects for electronic processing," Appl. Opt. **31,** 2438–2445 (1992).
11. B. Dhoedt, P. D. Dobbelaere, L. Buydens, P. Baets, and B. Houssay, "Optical free-space board-to-board interconnect: options for optical pathways," Appl. Opt. **31,** 5508–5516 (1992).
12. F. E. Kiamilev, "Programmable optoelectronic multiprocessors: design, performance and CAD development," Ph.D. dissertation (University of California, San Diego, La Jolla, Calif., 1992).
13. M. Murdocca, "Computer-aided design of digital optical computers using free-space interconnects," in *Optics in Complex Systems,* F. Lanzl, H. Preuss, and G. Weigelt, eds., Proc. Soc. Photo-Opt. Instrum. Eng. **1319,** 126–127 (1990).
14. A. Louri, "Optical content-addressable parallel processor: architecture, algorithms, and design concepts," Appl. Opt. **31,** 3241–3258 (1992).
15. G. N. Lawrence, "Optical design with physical optics using GLAD," in *1990 International Lens Design Conference,* G. N. Lawrence, ed., Proc. Soc. Photo-Opt. Instrum. Eng. **1354,** 126–133 (1990).
16. B. R. Irving, "A technical overview of code V version 7," in *Recent Trends in Optical Systems Design and Computer Lens Design Workshop,* R. E. Fischer and C. Londono, eds., Proc. Soc. Photo-Opt. Instrum. Eng. **766,** 285–293 (1987).
17. D. C. Sinclair, "Super-Oslo optical design program," in *Recent Trends in Optical Systems Design and Computer Lens Design Workshop,* R. E. Fischer and C. Londono, eds., Proc. Soc. Photo-Opt. Instrum. Eng. **766,** 246–250 (1987).
18. B. P. Zeigler, *Object Oriented Simulation with Hierarchical, Modular Models: Intelligent Agents and Endomorphic Systems* (Academic, San Diego, Calif., 1990), Chap. 1.
19. P. J. Kiviat, R. Villanueva, and H. M. Markowitz, *The Simscript II Programming Language* (Prentice-Hall, Englewood Cliffs, N.J., 1969).
20. *GLAD Theoretical Description Manual* (Applied Optics Research, Tucson, Ariz., 1992).
21. G. N. Lawrence, "Optical design and optimization with physical optics," in *1990 International Lens Design Conference,* G. N. Lawrence, ed., Proc. Soc. Photo-Opt. Instrum. Eng. **1354,** 15–22 (1990).
22. G. Keiser, *Optical Fiber Communications* (McGraw-Hill, New York, 1991), Chap. 5.
23. D. H. Hartman, "Digital high speed interconnects: a study of the optical alternative," Opt. Eng. **25,** 1086–1102 (1986).
24. J. Shamir, H. J. Caulfield, and R. B. Johnson, "Massive holographic interconnection networks and their limitations," Appl. Opt. **28,** 311–324 (1989).
25. A. S. Miller and A. A. Sawchuk, "Capabilities of simple lenses in a free space perfect shuffle," in *Optical Enhancements to Computing Technology,* J. A. Neff, ed., Proc. Soc. Photo-Opt. Instrum. Eng. **1563,** 81–92 (1991).
26. J. Shamir, "Fundamental limits of optical computing," in *Optics in Complex Systems,* F. Lanzl, H. Preuss, and G. Weigelt, eds., Proc. Soc. Photo-Opt. Instrum. Eng. **1319,** 168–172 (1990).
27. M. Govindarajan and S. R. Forrest, "Optically powered arrays for optoelectronic interconnection networks," Appl. Opt. **30,** 1335–1346 (1991).
28. T. V. Moui, "Receiver design for high-speed optical-fiber systems," J. Lightwave Technol. **LT-2,** 243–267 (1984).
29. J. L. Jewell, Y. H. Lee, A. Scherer, S. L. McCall, N. A. Olsson, J. P. Harbison, and L. T. Florez, "Surface-emitting microlasers for photonic switching and interchip connections," Opt. Eng. **29,** 210–214 (1990).